Novel aspects of the microstructure of Poly(ethylene oxide) as revealed by microhardness: influence of chain ends

F.J. Baltá Calleja, C. Santa Cruz[1]
Instituto de Estructura de la Materia, C.S.I.C., Serrano 119, Madrid 28006, Spain.

Abstract

The microhardness (H) of a series of melt crystallized samples of polyethylene oxide (PEO) was investigated as a function of molecular weight and crystallization temperature (T_c). It is shown that for a given molecular weight, H and the crystal hardness (H_c) increase with T_c, following a thermodynamic approach which takes into account the dependence of H_c upon crystal thickness (ℓ_c). A combined analysis of H–data and DSC results reveals that, both, the surface free energy (σ_e) and the hardness–derived parameter b of the samples is unaffected by T_c. The microhardness of the PEO samples was markedly affected by molecular weight. Furthermore, it is shown that the molecular weight variations produce changes on the surface free energy due to variations in the number of chain ends on the crystal surface, giving rise to a parallel variation in the b parameter. As a consequence, the melting temperature and the crystal hardness exhibit a similar dependence on crystal thickness.

1 INTRODUCTION

In recent years microhardness of semicrystalline polymers has been shown to be a property which can be directly related to their microstructure [1]– [5]. In preceding studies [6] Baltá and Kilian developed a theoretical model of deformation involving the energy dissipated by the plastically deformed crystals under the indenter, to account for the dependence of the crystal hardness on the average thickness ℓ_c of the crystal lamellae.

The hardness of the crystals is given by:

$$H_c = \frac{H_c^{\infty}}{1 + \frac{b}{\ell_c}} \tag{1}$$

[1]present address: Instituto de Ingeniería del Conocimiento, Universidad Autónoma de Madrid, Canto Blanco, Módulo C–XVI, P. 4, Madrid 28049, Spain.

where H_c^∞ is the hardness of an infinite crystal and b is a parameter which is proportional to the surface free energy of the crystals, σ_e,

$$b = \frac{2\sigma_e}{\Delta h} \tag{2}$$

Δh is the energy needed for plastic deformation of the crystals, involving the formation of a great number of shearing planes. Comparison of Eq. 1, accounting for the dependence of crystal hardness upon ℓ_c, with Young's dislocation model for yield has been recently shown to give good agreement for oriented polyethylene crystals [7]. The use of Eq. 1 has also been successfully used to establish the dependence of H_c upon ℓ_c of PEEK films [8].

We have previously pointed out [9] the existing analogy between Eq. 1 and the Thomson–Gibbs equation:

$$T_m = T_m^o \left(1 - \frac{2\sigma_e}{\Delta h_f^o \ell_c}\right) \tag{3}$$

This analogy permits to define a parameter $b^* = 2\sigma_e/\Delta h_f^o$, where Δh_f^o is the equilibrium enthalpy of fusion. Thus while the ratio b^* describes the melting point depression due to the finite thickness of the lamellae, the ratio b similarly describes the H_c depression owing to the finite dimension of the crystals.

In case of melt crystallized PE samples [9] the increase in the b–parameter with molecular weight was shown to be parallel to the increase in σ_e derived from DSC experiments. The increase in σ_e was interpreted in terms of an increase in the number of defects and molecular entanglements located onto the surface boundary of the lamellar crystals. Variations of H with composition in PE/PP gel blends have also been discussed in the light of changes occurring in the defective boundary of the lamellar crystals [10] In our previous studies on melt crystallized PE [9] the molecular weight range investigated was sufficiently high (56000–307000) as to assume that the chain ends had no effect on σ_e. The variations in σ_e were mainly ascribed to the increasing number in defects and molecular entanglements. On the other hand microhardness studies on short paraffins crystals reveal the influence of the molecular packing and hence, of the chain ends on the b–parameter [11].

There arises, as well, the possibility to examine the mechanical properties of long chain compounds in a molecular weight range, corresponding to materials, not yet classified as high polymers, as e.g. oligomers [12], in which the number of chain folds is comparable to the chain ends on the crystal surface. Within this molecular range, one may expect that chain ends play a relevant role in the contribution to the surface free energy variation when the molecular weight is changed.

The aim of this work is to investigate the microhardness of poly(ethylene oxide) samples (PEO) in the molecular weight range corresponding to the transition from straight chain crystallization of oligomers to the folded chain crystallization of polymers. The crystallization of melt crystallized PEO and the characterization of the

lamellar structure by SAXS was the object of an early study in which the effect of molecular weight on fold length was thorough investigated [13,14]. In the present work we wish to examine the influence of chain ends and chain folds, both, on the surface free energy as derived from DSC data using Eq. 3 and on the b parameter using Eq. 1.

Two routes will be followed: a) the crystal thickness (ℓ_c) of the PEO samples will be changed and the surface free energy of the crystals will be kept constant by an isothermal crystallization of a given sample at different temperatures, T_c. b) σ_e and ℓ_c will be changed simultaneously by changing the molecular weight of the samples. In this way, we will also derive the value of H_c^∞ and study the influence of T_c and molecular weight on the σ_e value.

2 EXPERIMENTAL

Table 1 shows the commercial name and the average number molecular weight (M_n) of the PEO grades investigated. The extended molecular length, $\lambda = M_n/\nu$ is also represented, where $\nu = 15.82\,\mathrm{g/\AA}$ is the molar mass per monomer unit length along the c axis [15]. It is noteworthy that these materials present low dispersity values (~ 1.2). Let us recall that, in contrast to the planar zig–zag structure of the PE crystalline molecules, the PEO molecules in the crystals show a 7/2 helical conformation with a period of 19.3Å and a monomer repeating length of 2.8Å[16]. Two different series of samples were investigated: In a first series the sample with $M_n = 13000$ was crystallized at different temperatures in the range of 30–58 °C for different crystallization times ranging between 1 and 72h. For the second series the materials collected in table 1 were used. In this case, the samples were melted 10 °C above the melting temperature and quenched in ice water from the molten state. All the samples were compression molded in the form of 2 mm thick films.

The density was measured in a gradient column using a mixture of toluene/carbon tetrachloride. The volume degree of crystallinity, α, was calculated from density values assuming values for the crystal density $\rho_c = 1.2267\,\mathrm{g/cm^3}$ and for the amorphous density $\rho_a = 1.1227\,\mathrm{g/cm^3}$ [13].

The melting temperature and enthalpy of fusion were obtained using a Perkin–Elmer DSC–4 differential scanning calorimeter. Scanning rates of 5, 10 and 15 °C/min were used. The melting temperature was obtained by extrapolation of the scanning rate to 0°C/min.

The SAXS measurements were carried out using a rotating anode Rigaku X–ray generator with a Kissig camera and a sample–film distance of 500 mm. The long period, L, was obtained applying Bragg's law to the maximum derived after subtraction of the background scattering and after performing the Lorenzt's correction. The crystal thickness, ℓ_c, was derived from the equation:

$$\ell_c = \alpha L \tag{4}$$

The microhardness measurements were carried out using a Leitz microindenter equipped with a Vickers diamond using a loading cycle of 0.1 min to minimize the creep behavior and different loads of 0.15, 0.25, 0.5 and 1 N. The microhardness value was obtained using the equation:

$$H = 1.854\frac{P}{d^2} \tag{5}$$

where P is the applied load, d is the length of the residual indentation in the material and the value of 1.854 is a factor which takes into account the geometry of the diamond. The crystal hardness, H_c, was calculated assuming $H_c \approx H/\alpha$.

3 RESULTS

3.1 Microhardness of PEO: Influence of the crystallization temperature

Table 2 collects the values of ρ, α, α_{DSC}, L, ℓ_c, H, H_c, T_m and n for the PEO sample with $M_n = 13000$ isothermally crystallized at different temperatures. In this table, n stands for the number of chain folds per chain in the crystals, $n + 1 = \lambda/\ell_c$.

Since in all cases n is an integer, the crystal thickness values (see table 2) correspond to structures in which the two chain ends of each molecule are located at the crystal surface.

Figure 1 shows the increasing parallel variation of α and α_{DSC} values for the sample with $M_n = 13000$ as a function of crystallization temperature (T_c). The discrepancy between α and α_{DSC} is lower than 3%. It is to be noted the large crystallinity values obtained for these samples, $\alpha > 90\%$. This is due to the low molecular weight of the sample investigated confirming the regular structure of crystals with mainly chain folds and chain ends at the surface boundary and little disordered material within the lamellae [13].

Figure 2 represents the variation of the long period, L, and of the crystal thickness, ℓ_c, for the sample with $M_n = 13000$ crystallized at different T_c. A discontinuous variation of L as well as ℓ_c is observed as reported earlier by Arlie et al. [13]. The reason for this stepwise variation is that chain ends are not located within the lamellar crystals but are rejected into the thin amorphous layers between crystals. For low crystallization temperatures $T_c \sim 30\,^{\circ}\mathrm{C}$ the molecules in the crystals present $n = 4$ folds. With increasing T_c the number of folds changes discontinously to 3 and 2, reaching finally a value of $n = 1$ for $T_c = 56\,^{\circ}\mathrm{C}$ (Table 2). This discontinuous variation can be observed because the extended molecular length, $\lambda = 822\,\text{Å}$ is sufficiently short as to give a crystal thickness increment proportional to an integer fraction of the molecular length [17,18].

Since the glass transition temperature of the PEO is well below room temperature [20], the contribution to the overall hardness value of the amorphous phase can be neglected, $H_a \approx 0$. Hence, the hardness value can be written as:

$$H \approx \alpha H_c \tag{6}$$

where α is the crystallinity and H_c is the crystal hardness. With these considerations in mind, the values of H and H_c as a function of T_c are represented in figure 3. In spite of the discontinuous ℓ_c variation observed in the range of $T_c = 30$–$55\,^{\circ}\mathrm{C}$, a more or less gradual increase of H_c as a function of T_c up to a value of $T_c = 55\,^{\circ}\mathrm{C}$ is obtained. At this temperature a discontinuous step in H_c is observed. This discontinuous variation is due to the large variation in the crystal thickness involving a transition from a crystal with $n = 2$ folds ($\ell_c = 230\,\text{Å}$) to crystals with $n = 1$ folds ($\ell_c = 375\,\text{Å}$). The rather continuous increase in H with T_c might be justified through the influence of the gradual increase of α with T_c shown in Fig. 1.

The surface free energy of the crystals, σ_e, can be obtained from the plot of the melting temperature, T_m, versus the reciprocal of the crystal thickness, $1/\ell_c$, as can be seen in figure 4. From the intercept and from the slope of this straight line values of $T_m^o = 341.9\,\mathrm{K}$ and $b^* = 2\sigma_e/\Delta h_f^o = 3.19\,\text{Å}$ are obtained. The value of T_m^o is in agreement with previous observation of Buckley and Kovacs [19]. On the other hand, the value of $\sigma_e \approx 38\,\mathrm{erg/cm^2}$ can be calculated from the b^* parameter using $\Delta h_f^o = 2.41 \times 10^9\,\mathrm{erg/cm^3}$ [19]. This value is somewhat larger than the value previously obtained ($\sigma_e = 27 - 30\,\mathrm{erg/cm^2}$ [17]). This discrepancy be due to the difference in the molecular weight between our sample and those from Buckley and Kovacs. From the above data (Figure 4) one can conclude that the surface free energy of the crystals remains nearly constant in the range of crystallization temperature investigated.

3.2 Influence of molecular weight upon hardness

Table 3 collects the values of ρ, α, α_{DSC}, L, ℓ_c, H, H_c, T_m and n for the PEO samples investigated as a function of molecular weight, M_n. Figs. 5a and b represent the variation of the volume degree of crystallinity and of L and ℓ_c as a function of M_n. As expected, one sees a rapid increase of α, L and ℓ_c for low molecular weights, and a leveling off tendency for $M_n \sim 2 \times 10^3$. It is to be noted the good agreement obtained between α and α_{DSC} values. For $M_n > 2 \times 10^4$ a slight crystallinity decrease is observed. This decrease maybe due to the increase in viscosity with increasing molecular weight which hampers the crystallization from the melt. Inspection of Fig. 5b shows that for low molecular weight values the chains are totally extended in the crystals, $n = 0$, (compare with table 3). On the other hand, With increasing molecular weight the number of chain folds in the crystals increases (Table 3).

Figure 6 represents the variation of H and H_c as a function of molecular weight. For low molecular weights the H values are extremely low ($H \approx 3\,\mathrm{MPa}$). However, H increases with M_n up to a maximum of $H \sim 65\,\mathrm{MPa}$ value for $M_n \sim 2 \times 10^4$ from which the hardness value decreases again. The variation obtained in H with M_n approximately follows the changes observed in crystallinity and crystal thickness.

It is to be noted that with increasing molecular weight there is a transition from extended chains to chain folded crystals (Fig. 5b). This transition must dramatically affect the surface free energy of the crystals. As pointed out previously [17,21], when the crystals have extended chains there is a high proportion of hydrogen bond formation between the -OH groups at adjacent chain ends. These bonds should provide high surface free energy values. On the other hand, with increasing number of chain folds the density of H–bonds at the lamellar surface diminishes and the surface free energy tends towards energy values required for the bending of a chain. The surface free energy value in this case should be considerably lower, due to the high flexibility of the PEO chains [19]. This variation in the surface free energy should be reflected in the plots of T_m and H_c versus $1/\ell_c$, in accordance with Eqs. 1 and 3. Figure 7a illustrates the variation of T_m versus $1/\ell_c$, clearly showing a decrease in the slope for each sample with increasing number of folds. Table 3 collects the values of σ_e derived from Eq. 3 for the various samples.

Figure 7b depicts the variation of H_c against $1/\ell_c$, showing different curves for the samples with different n values. In these two plots it is seen that, samples with the same number of chain folds have a surprisingly similar behavior in their representation of T_m or H_c against $1/\ell_c$. Furthermore, the slope (curvature) in the variation of T_m (H_c) versus $1/\ell_c$ diminishes with increasing number of chain folds to a limiting value ($n = 4$) from which the slope increases again up to $n = 6$ (sample with the highest molecular weight).

4 DISCUSSION

4.1 Crystal thickness dependence of H_c

The DSC results of Fig. 4 reveal that despite the fact that in the PEO samples crystallized at different T_c the number of folds is small (n = 1–4) the surface free energy has a constant value. This is due to the relatively high molecular weight of this sample which prevents OH chain ends to be active in hydrogen bond formation. This result is in accordance with the theoretical work of Buckley and Kovacs [17] which predicts that for $n > 1$ and high molecular weight, the influence of chain ends on σ_e is negligible. If σ_e =const, a plot of $1/H_c$ versus $1/\ell_c$ should, therefore, give an straight line with an slope of b/H_c^∞ and the intercept equal to $1/H_c^\infty$. Figure 8 shows the plot of $1/H_c$ against $1/\ell_c$ where a straight line is obtained. From this straight line, values of $b = 270$ Å and $H_c^\infty = 150$ MPa are deduced. The constancy obtained for the b–parameter is consistent with the constant σ_e value obtained. If one compares the values of the mechanical parameter $b = 2\sigma_e/\Delta h$ and the thermodynamical parameter $b^* = 2\sigma_e/\Delta h_f$ one obtains that:

$$\Delta h_f^\circ \approx 90\Delta h \tag{7}$$

This means that the energy required for crystal fusion (Δh_f°) is much larger than

the energy for plastic deformation of the crystals. A similar result was obtained for melt crystallized PE lamellae although for PE the ratio $\Delta h_f^o/\Delta h$ was much smaller [9]. This difference suggest that the energy for crystal destruction in PEO is smaller than in PE. From the above results we can conclude that the dependence of H_c upon ℓ_c described by Eq. 1, is valid for melt crystallized PEO.

4.2 Molecular weight dependence of b

The results of table 3 show the obtained substantial variation of σ_e with M_n corresponding to the transition from straight chain structures ($n = 0$) to the chain folded morphology ($n \neq 0$) in which chain ends are progressively substituted by chain folds in the crystal surfaces ($n \neq 0$). It is interesting to note that the σ_e values obtained for the highest molecular weight sample are in accordance with the theoretical data derived by Buckley and Kovacs [17].

The decrease of surface free energy with increasing chain folds, can be interpreted by assuming that hydrogen bonds at the surface of the crystals are progressively substituted by chain folds [17]. However, for the highest molecular weight sample with $n = 6$, where no hydrogen bond formation is expected, the value of σ_e shows up an increase with respect to the samples with $n = 2$ and $n = 4$. One could speculate that this result might be in accordance with a rise in the number of defects and molecular entanglements with increasing molecular weight, as previously observed [9] in PE samples.

Table 3 shows, in addition, that in crystalline lamellae with extended chains ($n = 0$), the surface free energy has nearly a constant value which corresponds to a straight line in figure 7a and to a constant value for the b parameter in figure 7b. With increasing molecular weight the number of chain folds increases and the surface free energy diminishes, leading to two families of curves shown in figures 7a and 7b. Now one sees that the similar variation T_m and H_c with $1/\ell_c$ is due to the same variation in σ_e of the crystals with increasing molecular weight.

Let us next compare the variation of the b and b^* parameters with molecular weight (see table 4) and analyze the relationship, b/b^* between them. The values of b and b^* are represented in figure 9 as a function of M_n. The initial decrease in b^* is confirmed by a similar decrease of b with increasing molecular weight. Fig. 9 also confirms the minimum value of b similar to b^* for a molecular weight of $M_n \sim 10^4$.

It is noteworthy that the ratio b/b^* does not remain constant as in the case of the samples crystallized at different temperatures; it diminishes with increasing molecular weight. The reason for it is that the b parameter diminishes faster with M_n than the b^* parameter. Since the σ_e value is admittedly the same for both parameters b and b^*, the different variation of these parameters with M_n must be originated in the different variation of Δh and Δh_f^o with M_n. As Δh_f^o should have a constant value which is independent of M_n the observed varying b/b^* ratio must be due to changes occurring in Δh. One possible explanation for this effect might be sought

in the occurrence of tie molecules between adjacent crystals. Tie molecules may be expected to appear with increasing molecular weight, thus providing a reinforcement of the material which could contribute to an increase in the energy of destruction (Δh), and lead consequently to a b decrease. On the other hand, the tie molecules should not affect the thermodynamical parameter b^*. With these considerations in mind one can conclude that the b-parameter exhibits two different decreasing contributions in the molecular weight range between 10^3 and 10^4: first a contribution to an increasing Δh owing to the presence of tie molecules and, second, a contribution through the increase in the number of chain folds with increasing M_n.

5 CONCLUSIONS

Experiments performed on commercial PEO samples suggest that microhardness can be correlated with some morphological features. The study has shown the following:

1. A correlation between crystal hardness and lamellar thickness, following previous thermodynamic predictions [6] has been shown to apply for melt crystallized PEO in a wide range of molecular weights (10^3–10^5).

2. It is found that the mechanically derived b–parameter decreases in the range of PEO in which a transition from chain extended to chain folded crystal lamellar occurs. Analysis of DSC results reveals that such a decrease is parallel to a decrease in the σ_e value. It is suggested the influence of chain ends, involving hydrogen bond formation, to explain the high σ_e value.

3. It is shown that the b–parameter increases for high molecular weight samples and it is suggested that the σ_e rise is a consequence of the increasing number of defects and entanglements.

4. For sufficiently high molecular weight PEO the parameter b (and consequently σ_e) does not depend on the temperature of crystallization because the influence of chain ends on σ_e is negligible, even when the number of chain ends and the chain folds is comparable.

6 Acknowledgments

Grateful acknowledgment is due to the Comision Interministerial de Ciencia y Tecnología (Grant MAT90–0795) Spain for the generous support of this investigation.

References

[1] Baltá Calleja F.J., Adv. Polym. Sci. **1985**, *66*, 117

[2] Darlix B., Monasse B., Montmitonnet P., Polym. Testing **1986**, *6*, 107

[3] Lorenzo V., Pereña J.M., Fatou J.M., Mendez J.A., Arnaiz J.A., J. Mater. Sci. Lett. **1987**, *6*, 756

[4] Bajpai R., Keller J.M., Datt S.F., Makromol. Chem., **1988**, *20/21*, 465

[5] Evans B.L., J. Mater. Sci. **1989**, *24*, 173

[6] Baltá Calleja F.J., Kilian H.G., Coll. & Polym. Sci. **1988**, *266*, 29

[7] Santa Cruz C., Baltá Calleja F.J., Asano T., Ward I. M., Phil. Mag. **1993**, *A 68*, 209

[8] Deslandes Y., Alva Rosa F., Brisse F., Meneghini T., J. Mater. Sci. **1991**, *26*, 2769

[9] Baltá Calleja F.J., Santa Cruz C., Bayer R., Kilian H.G., Colloid & Polym. Sci. **1990** , *268*, 440

[10] Baltá Calleja F.J., Santa Cruz C., Asano T., Sawatari C., Macromolecules, **1990**, *23*, 5352

[11] Ania F., Kilian H.G., Baltá Calleja F.J., J. Mater. Sci. Lett. **1986**, *5*, 1183

[12] Baltá Calleja F.J., Keller H.H., J. Polym. Sci. **1964**, *2*, 2171

[13] Arlie J.P., Spegt P., Skoulios A.. Makromol. Chem. **1967**, *104*, 212

[14] Arlie J.P., Spegt P., Skoulios A.. Makromol. Chem. **1966**, *99*, 160

[15] Takahashi Y., Tadokoro H., Macromolecules **1973**, *6*, 672

[16] Tadokoro H., Chatani Y., Yoshihata T., Tahara S., Murahashi S. Makromol. Chem. **1964**, *73*, 109

[17] Buckley C.P., Kovacs A.J., Coll. & Polym. Sci. **1976**, *254*, 695

[18] Galin J.C., Spegt P., Suzuli S., Skoulios A., Makromol. Chem. **1974**, *175*, 991

[19] Buckley C.P., Kovacs A.J., Progr. Coll. & Polym. Sci. **1975**, *58*, 44

[20] Wunderlich B., ATHAS 5th Report, University of Tenessee, **1989**

[21] Baltá Calleja F.J., Hosemann R., Wilke W., J. Polym. Sci.: Part C, **1969**, *16*, 4329

[22] Flory P.J., Vrij A.. J. Am. Chem. Soc. **1963**, *85*, 3548

Commercial name	M_n	λ(Å)
Carbowax 1000	1000	63
Hoechst 1300	1300	82
Hoechst 2000	2000	126
Carbowax 4000	3500	221
Carbowax 6000	6700	423
Hoechst 13000	13000	822
Carbowax 20M	17000	1075

Table 1: *Poly(ethylene oxide) samples investigated as a function of molecular weight, M_n, and the extended chain length, λ.*

T_c (°C)	t_c (h)	ρ (g/cm^3)	α	α_{DSC}	L (Å)	ℓ_c (Å)	H (MPa)	H_c (MPa)	T_m (K)	n
30	1	1.2163	0.900	0.881	175	157	45	50	335.5	4
35	1	1.2174	0.911	0.876	175	159	51	56	336.0	4
40	1	1.2185	0.921	0.905	180	166	54	58	336.2	4
43	1	1.2187	0.923	0.901	205	184	56	60	336.5	3
45	1	1.2195	0.931	0.905	205	191	57	61	336.9	3
47	1	1.2202	0.937	0.911	207	194	59	63	336.7	3
49	1	1.2206	0.941	0.925	210	197	62	66	337.0	3
51	1	1.2210	0.945	0.934	250	236	64	67	337.3	2
53	1	1.2215	0.950	0.968	252	239	66	69	338.2	2
54	1	1.2219	0.953	0.981	248	236	72	75	338.0	2
55	3	1.2223	0.958	0.989	246	235	72	75	338.8	2
56	14	1.2226	0.961	0.987	390	375	86	90	339.2	1
57	24	1.2228	0.963	0.991	385	371	93	96	338.8	1
58	72	1.2236	0.971	0.987	385	373	97	98	339.2	1

Table 2: *Experimental values for the crystallization temperature, T_c, the crystallization time, t_c, density, ρ, crystallinity measured by density, α, crystallinity measured by DSC, α_{DSC}, long period, L, crystal thickness, ℓ_c, microhardness, H, crystal hardness, H_c, melting temperature, T_m, and number of chain folds per molecule, n, for the PEO sample with a molecular weight of $M_n = 13000$.*

M_n	ρ (g/cm^3)	α	α_{DSC}	L (Å)	ℓ_c (Å)	H (MPa)	H_c (MPa)	T_m (K)	σ_e (erg/cm^2)	n
1000	1.2064	0.804	0.78	73	59	3	3.2	310.3	65.7	0
1300	1.2132	0.870	0.85	80	70	4	4.5	316.1	63.6	0
2000	1.2159	0.896	0.87	132	118	9	10.0	326.9	62.4	0
3500	1.2161	0.898	0.88	140	126	23	25.4	331.3	47.4	1
6700	1.2169	0.906	0.91	155	140	53	58.0	335.0	34.3	2
13000	1.2184	0.921	0.91	165	152	59	63.7	336.0	31.7	4
17000	1.2183	0.895	0.89	147	135	43	47.7	333.4	40.7	6

Table 3: *Experimental values for the density, ρ, crystallinity measured by density, α, crystallinity measured by DSC, α_{DSC}, long period, L, crystal thickness, ℓ_c, microhardness, H, crystal hardness, H_c, melting temperature, T_m, surface free energy, σ_e, and the number of chain folds per molecule for the PEO samples with different molecular weights.*

M_n	b(Å)	b^*(Å)	b/b^*
1000	2706	5.4	501
1300	2263	5.2	435
2000	1652	5.1	323
3500	618	3.9	158
6700	222	2.8	79
13000	206	2.6	79
17000	290	3.4	85

Table 4: *Calculated values for the b and b^* parameters and the ratio between them as a function of molecular weight, M_n.*

Legend to Figures

Figure 1: Variation of the volume degree of crystallinity measured by density, α (o) and the by DSC, α_{DSC} (•) as a function of crystallization temperature, T_c.

Figure 2 Variation of long period, L (o) and crystal thickness, ℓ_c (•) as a function of T_c.

Figure 3 Variation of microhardness, H (o) and crystal hardness, H_c (•) as a function of T_c.

Figure 4 Plot of the melting temperature of the crystals, T_m, as a function of the reciprocal crystal thickness for the sample crystallized at different temperatures.

Figure 5 a) Variation of the volume degree of crystallinity, α, as a function of the molecular weight, M_n. (o) Crystallinity measured by density. (•) Crystallinity measured by DSC. b) Variation of the long period, L (o), and crystal thickness, ℓ_c (•) and extended chain length (dashed–line) as a function of molecular weight.

Figure 6 Variation of experimental values of H (o) and H_c (•) as a function of molecular weight, M_n.

Figure 7 a) Plot of T_m as a function of $1/\ell_c$ for the PEO samples with different molecular weights. b) Variation of H_c as a function of $1/\ell_c$ for PEO samples with different molecular weights.

Figure 8 Variation of the reciprocal crystal hardness, $1/H_c$, as a function of the reciprocal crystal thickness, $1/\ell_c$, for the PEO with $M_n = 13000$ sample crystallized at different temperatures.

Figure 9 Variation of b and b^* parameters as a function of molecular weight, M_n.

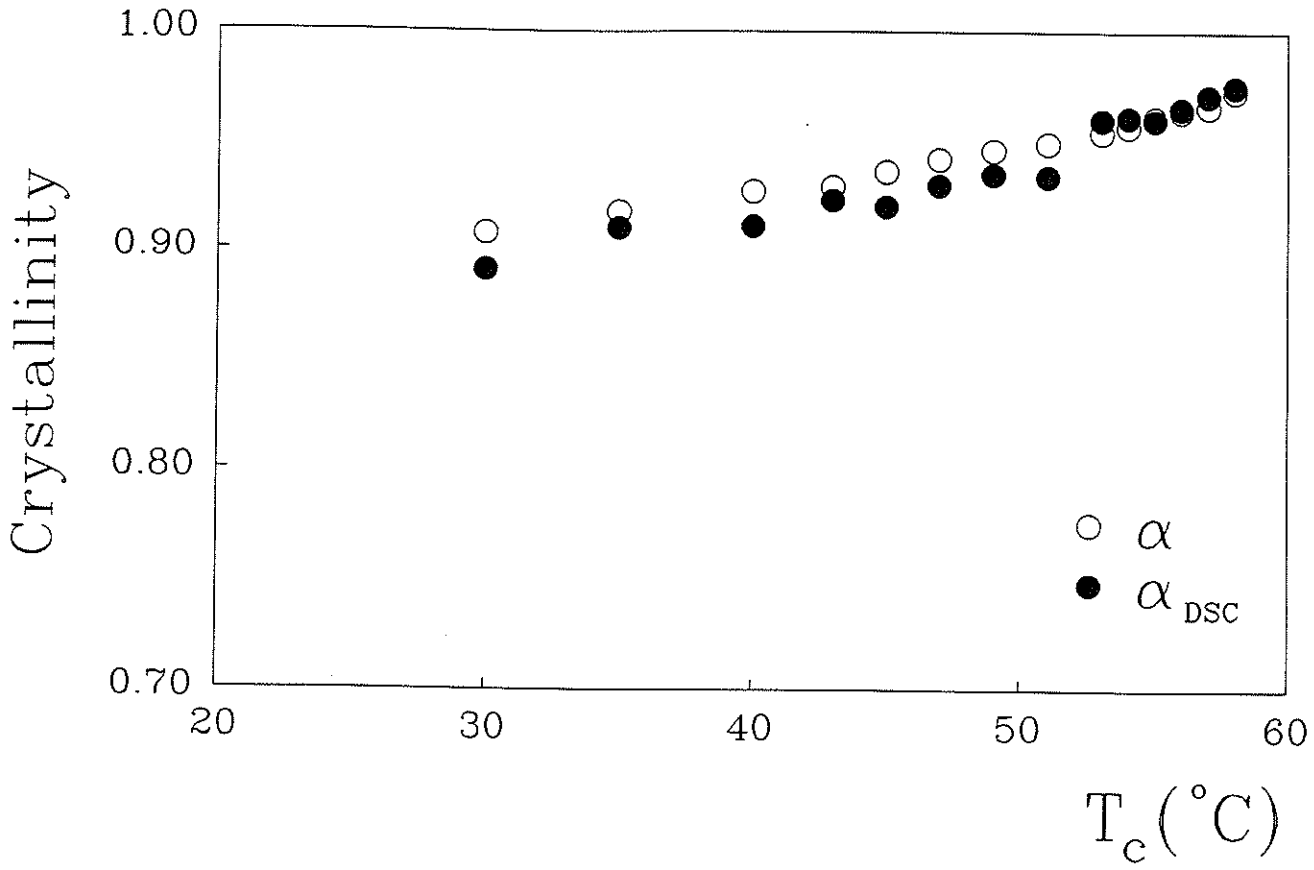

Fig. 1

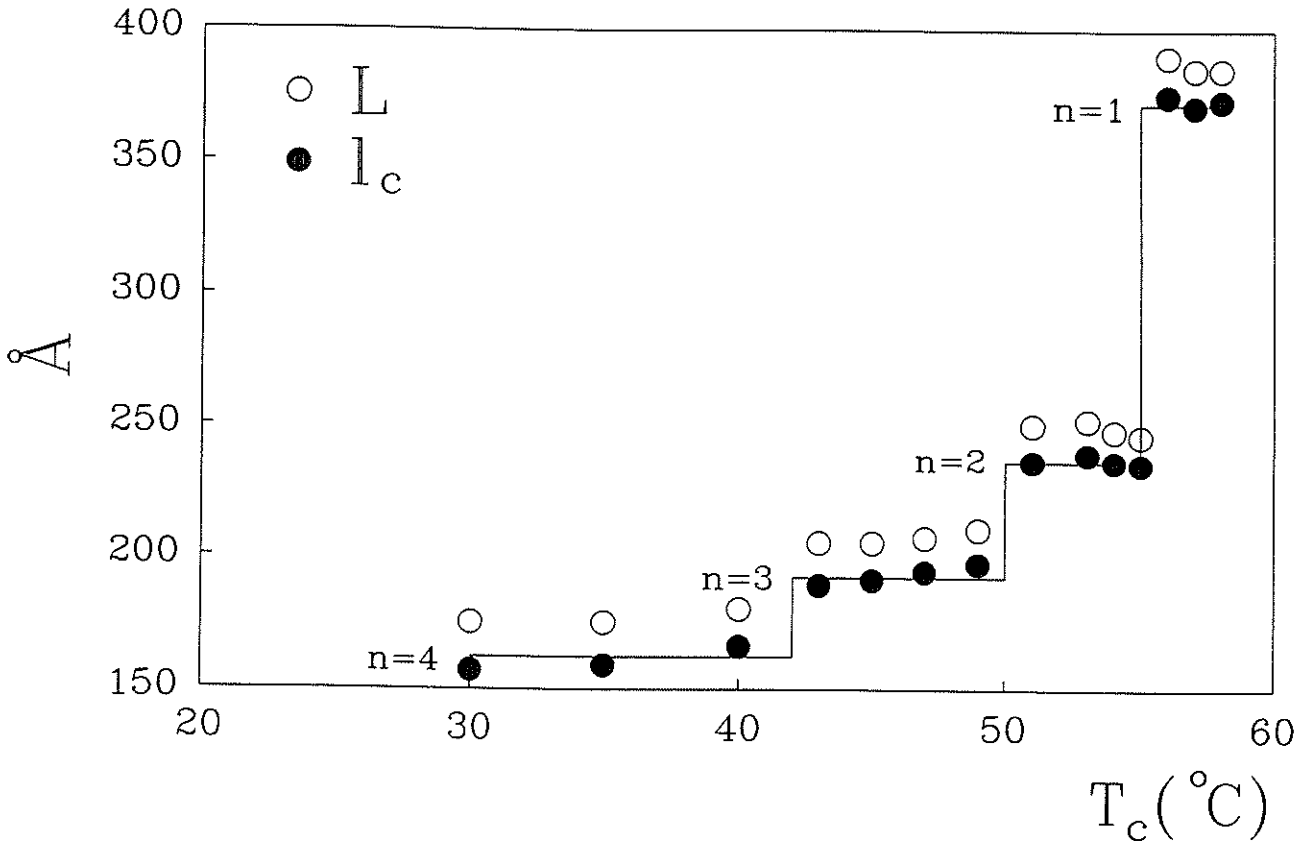

Fig. 2

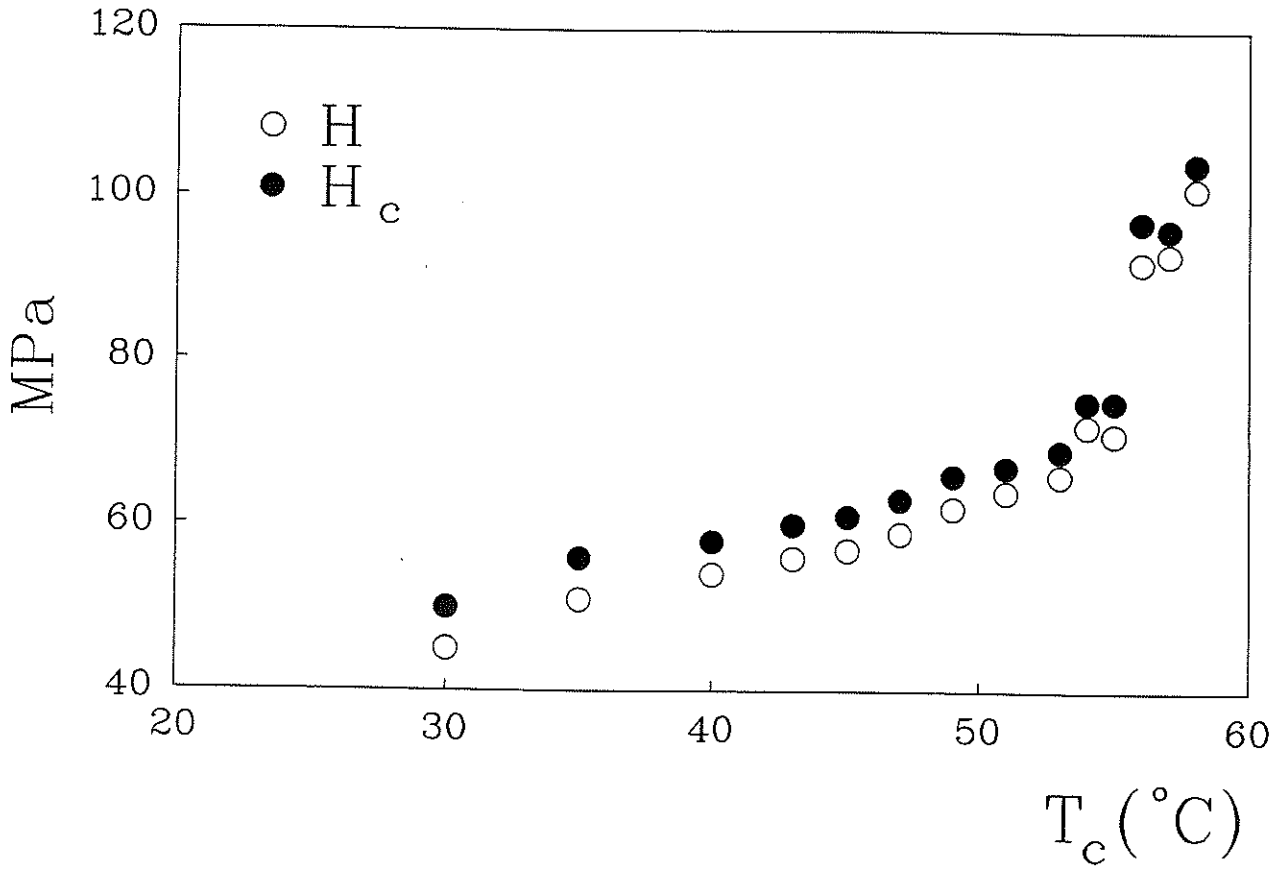

Fig. 3

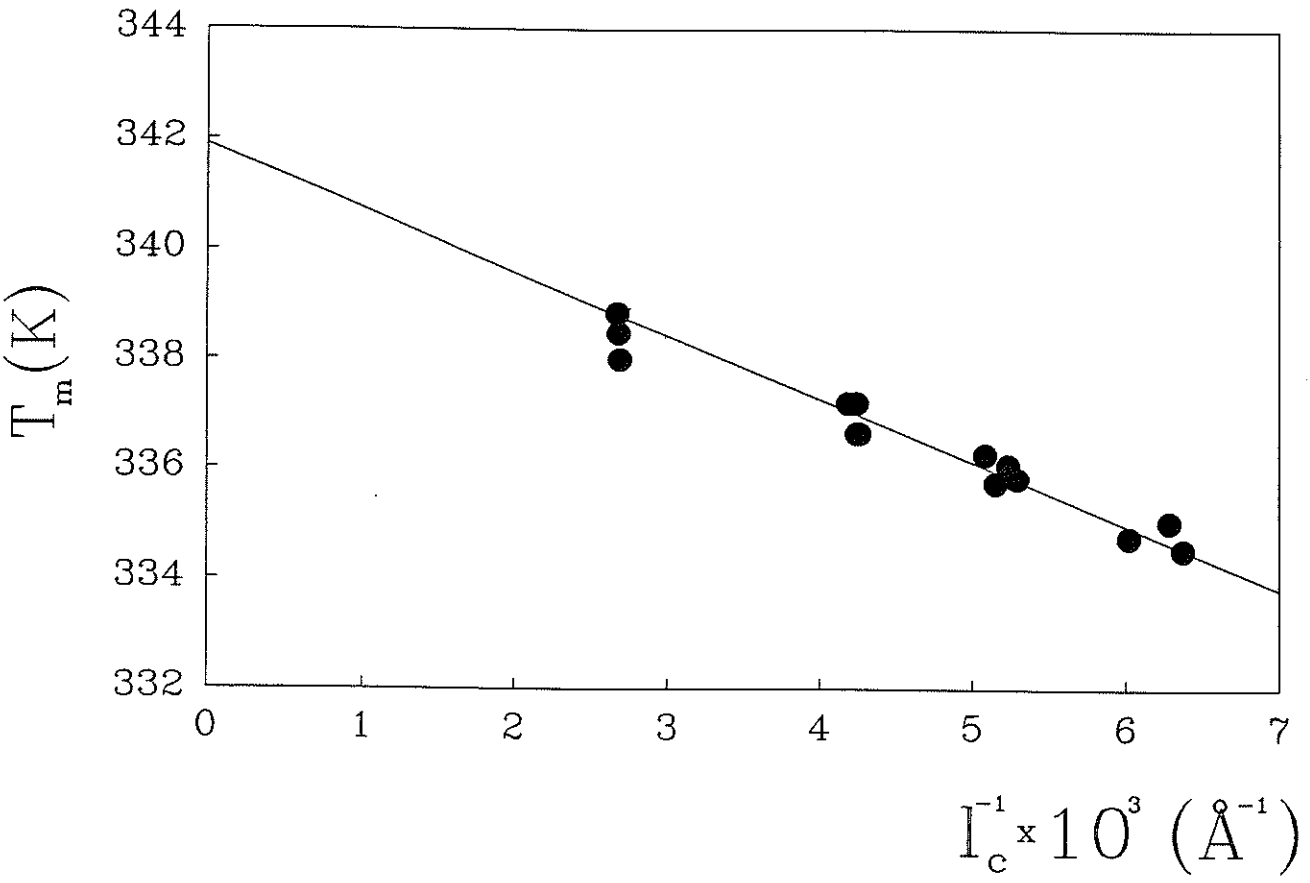

Fig 4

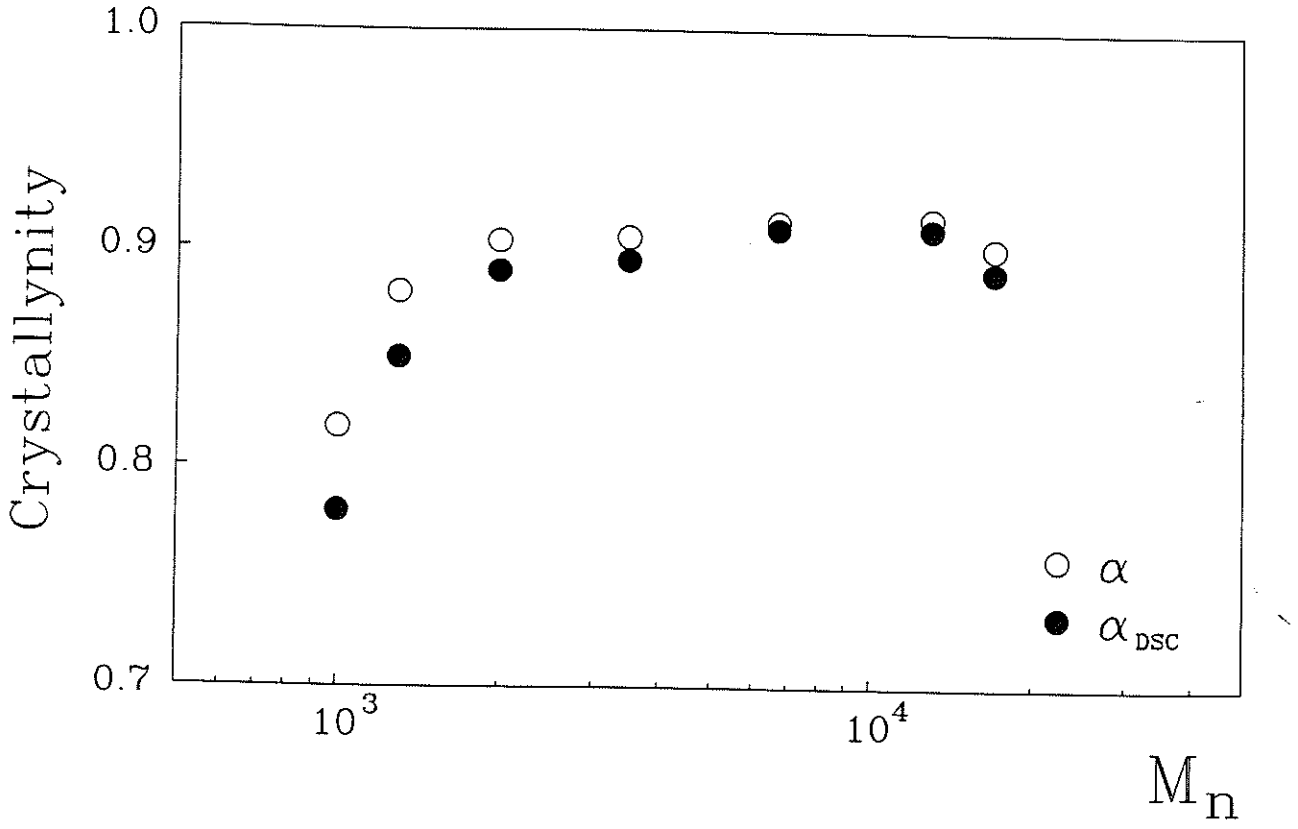
1.0
0.9
0.8
0.7
Crystallynity
α
α DSC
10^3
10^4
M_n

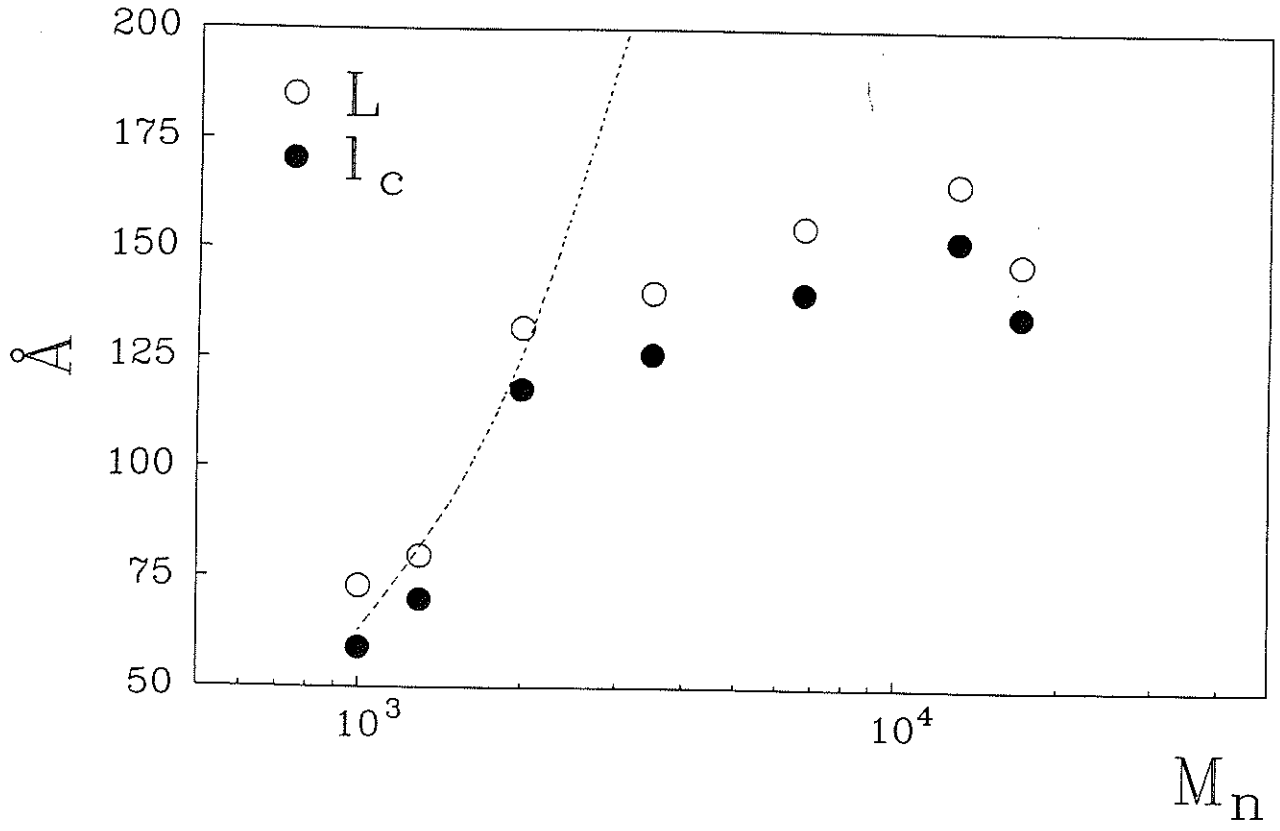
200
175
150
125
100
75
50
Å
L
l c
10^3
10^4
M_n

Fig. 5

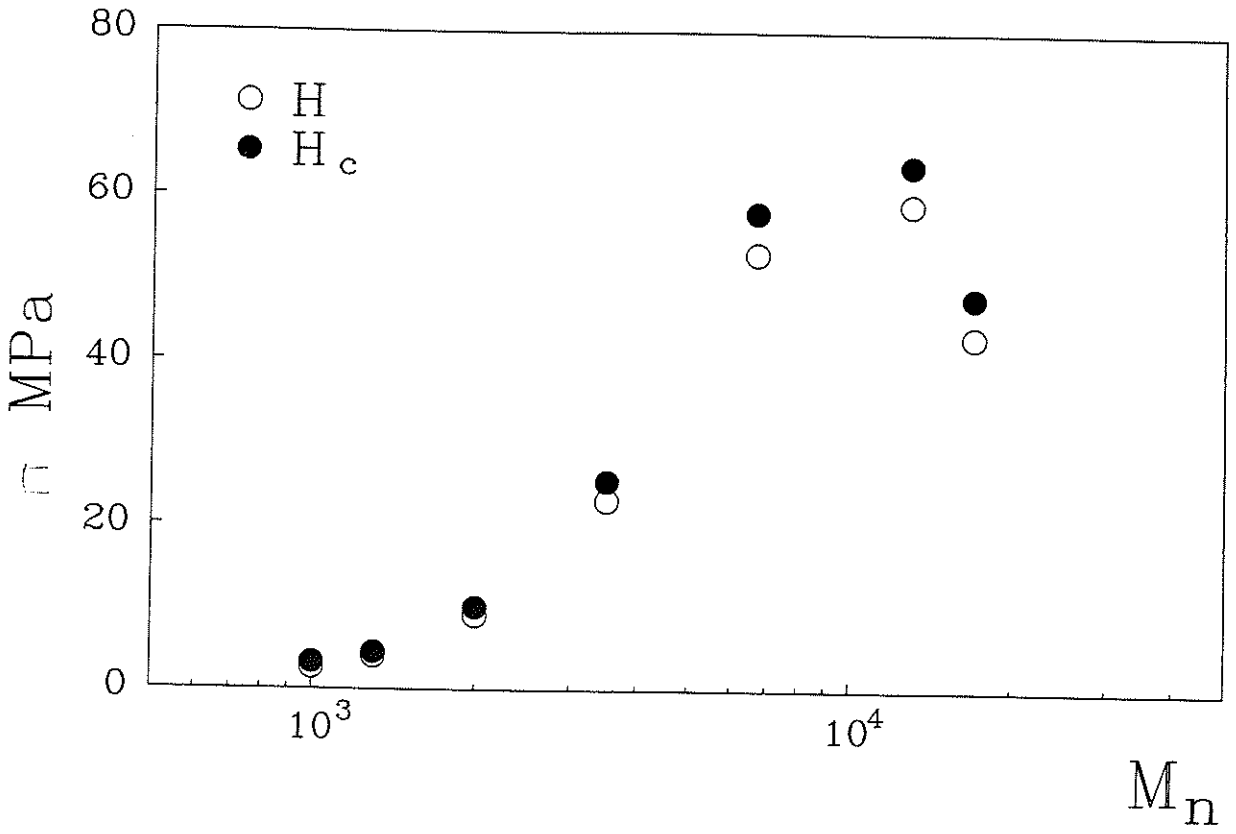

Fig 6

a)

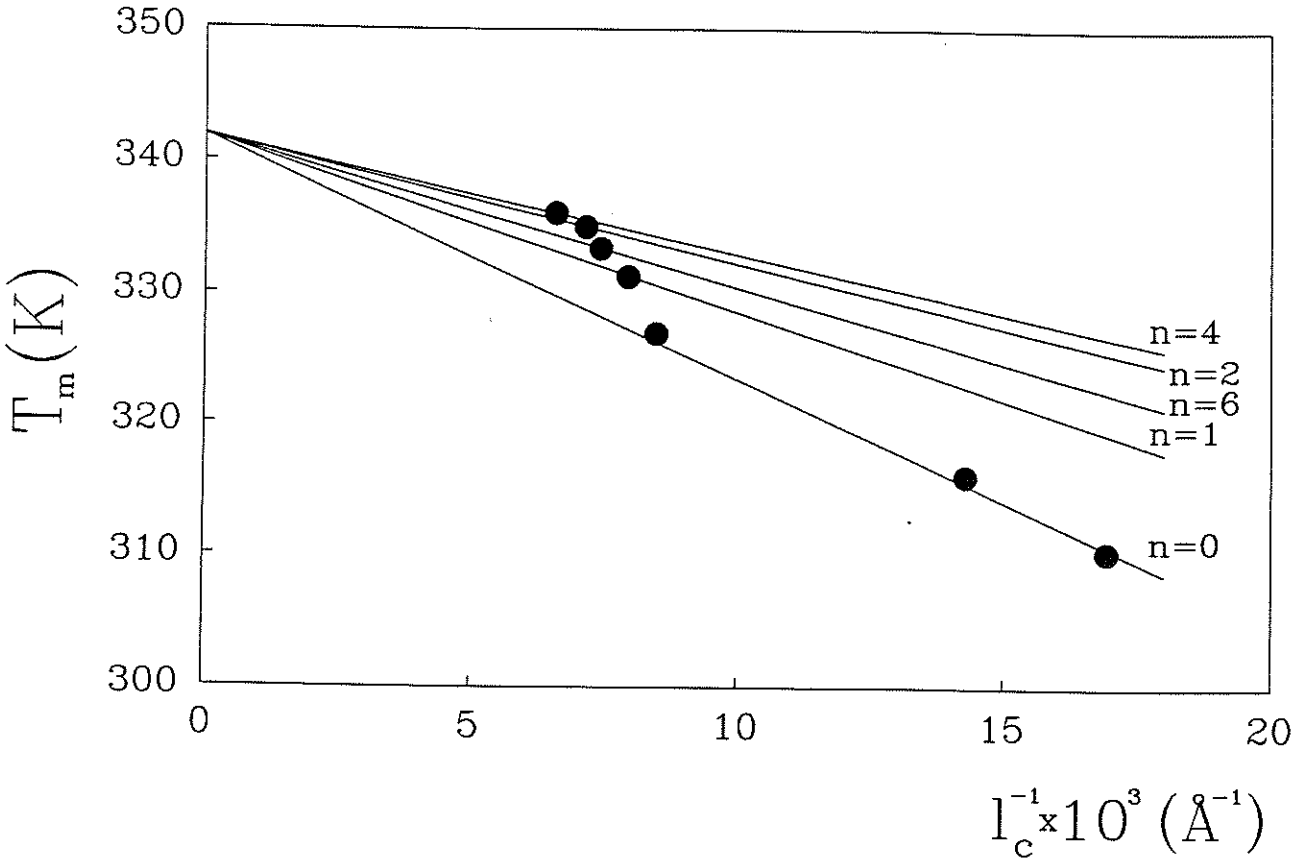
350
340
330
320
310
300
T_m (K)
0
5
10
15
20
$l_c^{-1} x 10^3$ (Å^{-1})
n=4
n=2
n=6
n=1
n=0

b)

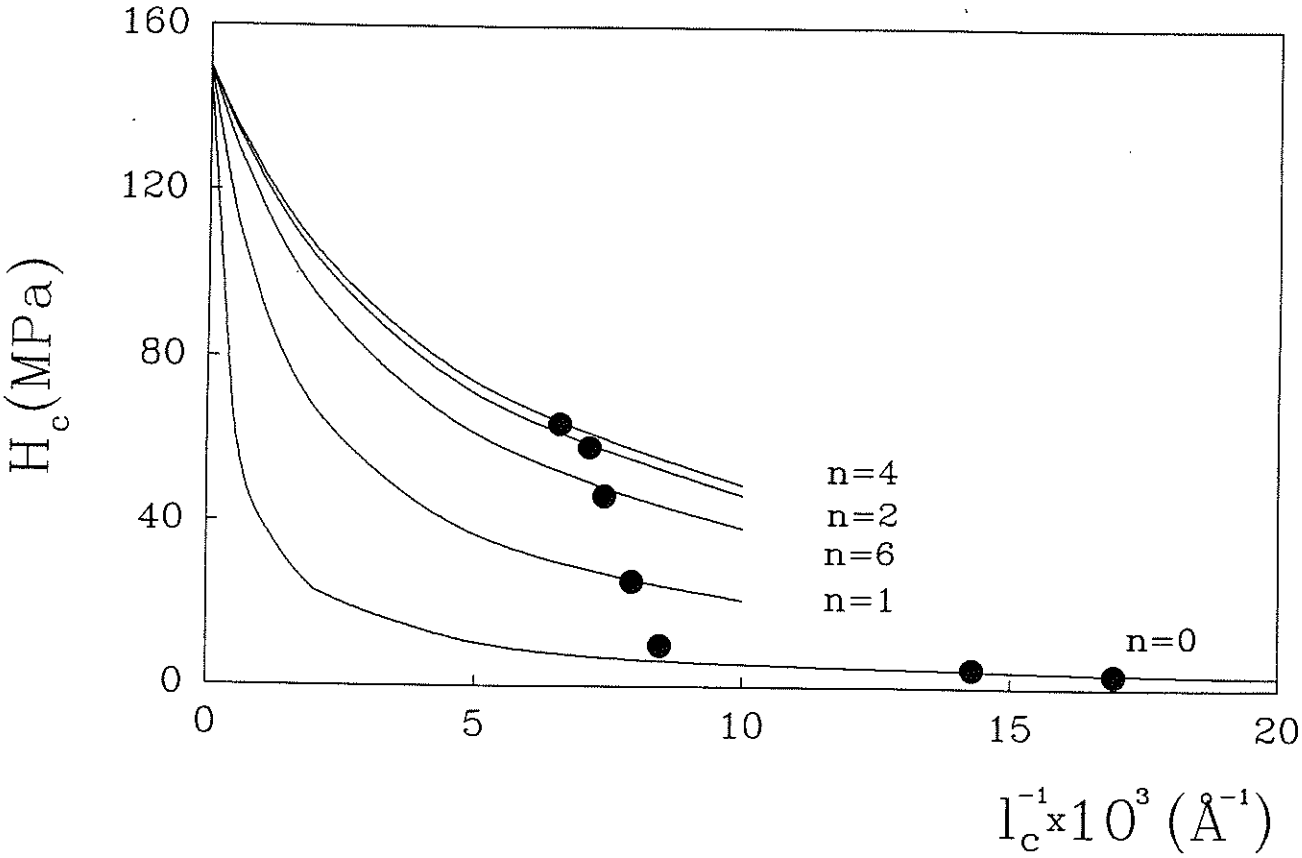
160
120
80
40
0
H_c (MPa)
0
5
10
15
20
$l_c^{-1} x 10^3$ (Å^{-1})
n=4
n=2
n=6
n=1
n=0

Fig. 7

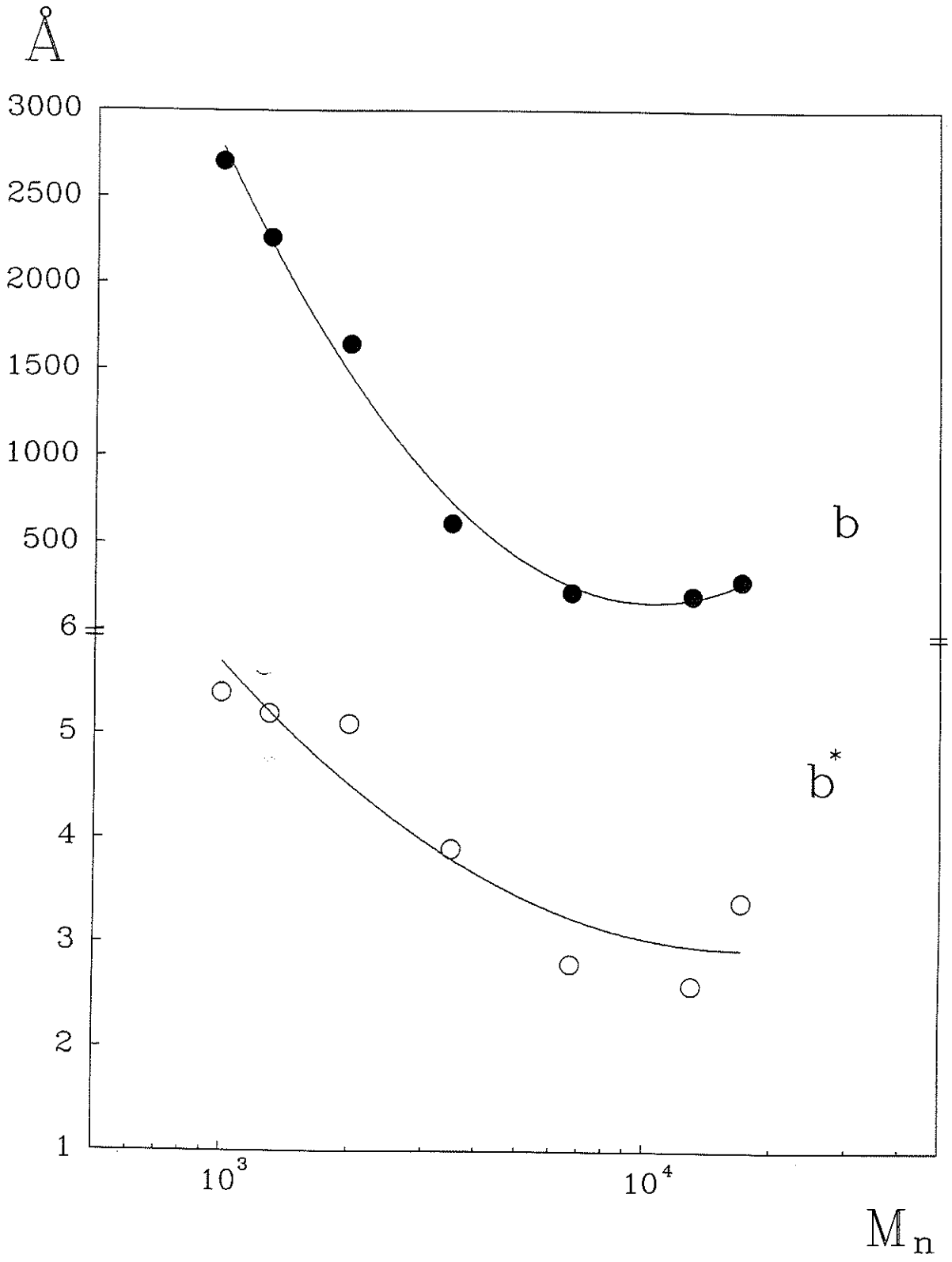

Fig. 9

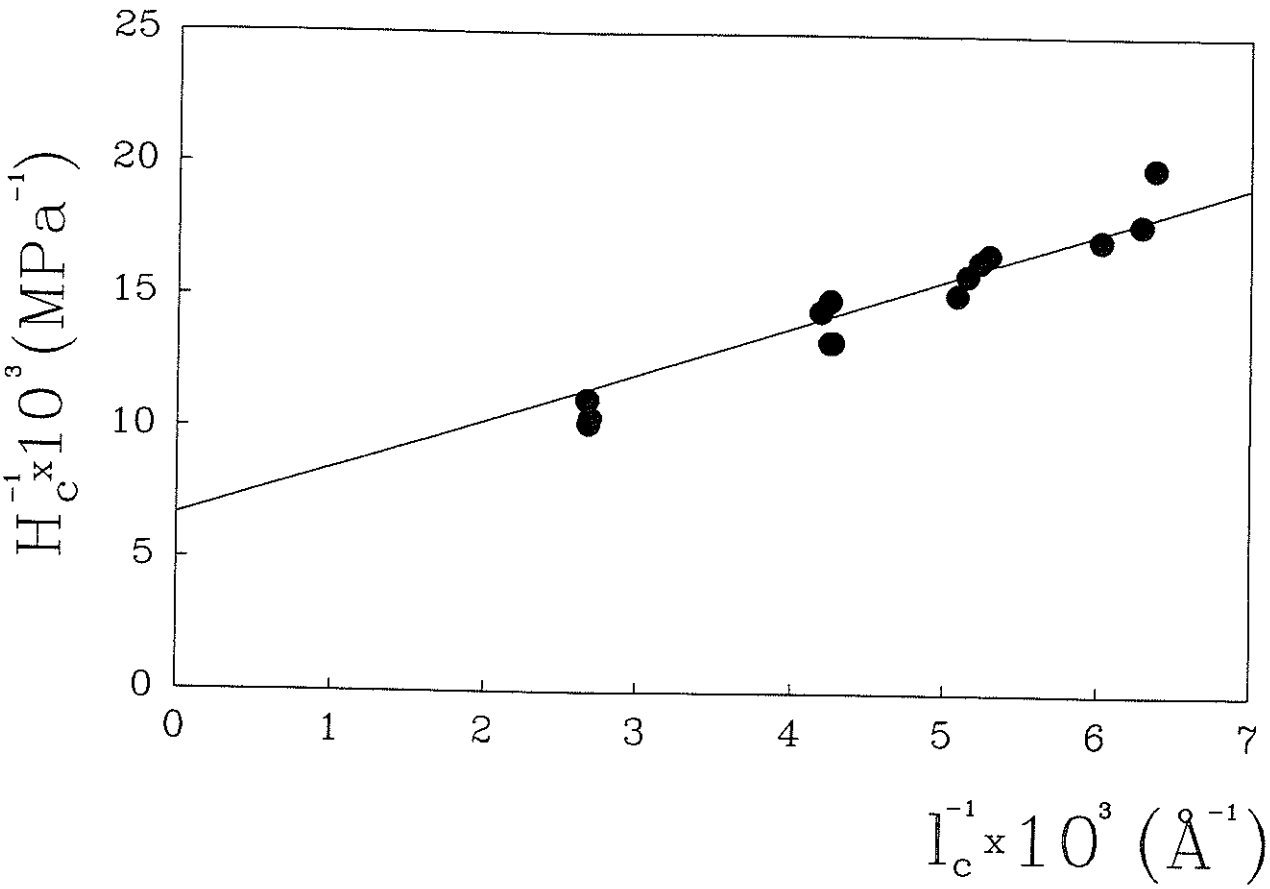

Fig. 8

POL/940094

p.2, l 1 "infinity" : infinite?

p.2, l 4 "plastic destruction" : please explain what this means.

equt. 2 define σ_e in text.

equt. 4 define α in text.

fig. 9 label on y axis required.

General points

Error bars are required to justify, in particular, the validity of fig.9.

$$\frac{2\nu}{Dh_f^0}$$

$$\frac{t_c(T_m^0 - T_m)}{T_m^0} = b^*$$

$$\frac{\Delta b}{b} \sim 5\% \qquad \frac{\Delta H}{H} \sim 5\%$$

$$\frac{\Delta b^*}{b} \sim 1\%$$